Journal of Solid State Chemistry 183 (2010) 3023–3028

Contents lists available at ScienceDirect

Journal of Solid State Chemistry

journal homepage: www.elsevier.com/locate/jssc

Crystal, electronic structure and electronic transport properties of the $Ti_{1-x}V_xNiSn$ ($x=0$–0.10) solid solutions

Yu. Stadnyk [a], A. Horyn' [a], V.V. Romaka [a], Yu. Gorelenko [a], L.P. Romaka [a], E.K. Hlil [b,*], D. Fruchart [b]

[a] Ivan Franko National University of Lviv, Kyrila and Mefodiya str., 6, 79005 Lviv, Ukraine
[b] Institut Néel, CNRS, Université Joseph Fourier, BP 166, 38042 Grenoble, France

ARTICLE INFO

Article history:
Received 4 July 2010
Received in revised form
29 August 2010
Accepted 26 September 2010
Available online 20 October 2010

Keywords:
Half-Heusler phases
Electrical resistivity
Seebeck coefficient
Electronic structure calculations

ABSTRACT

The *n*-TiNiSn ternary intermetallic semiconductor is doped by the V donor impurity and the crystalline structure of the obtained $Ti_{1-x}V_xNiSn$ solid solutions ($x=0$–0.10) is determined by X-ray diffraction. Temperature and concentration dependences of the resistivity and thermopower are investigated in 80–380 K range. As main results, the TiNiSn conductivity type is revealed insensitive to V doping and the thermopower factor substantially increases versus V content. First principle calculations based on DFT using FPLO and KKR–CPA methods are performed as well. Experimental data and electronic structure calculations are compared and discussed in terms of thermopower improvements.

1. Introduction

Equiatomic TiNiSn, ZrNiSn, and HfNiSn compounds with the MgAgAs crystal structure type (ST), called *half-Heusler phase,* are formed in the *M*–Ni–Sn (*M*=Ti, Zr, Hf) metallic systems [1–3]. Despite these compounds are formed with the metallic elements, previous works on electron transport, optical and resonance properties point out to their semiconductor character [4–6]. Partial substitution enables to modify their transport properties and create thermoelectric materials with predictable parameters for technical applications.

Doping of the basic ternary compounds of the MgAgAs structure type (ST), in particular, TiNiSn, ZrNiSn or HfNiSn, allows to considerably improve the power factor value of Z^* ($Z^*=S^2\cdot\sigma$, where S is the thermopower and σ the electrical conductivity) [7–10]. Partial substitution of the constituents in various crystallographic positions of the MgAgAs structure type (ST) materials was previously reported, however Z^* values are not yet determined for these compounds type.

In previous works [5,11–13], we analyzed the effect of heavy doping of the intermetallic compounds with the MgAgAs-type by acceptor or donor impurities. We examined, particularly, the energy bands and crystalline structure changes upon doping nature. Electronic transport, magnetic and optical characteristics were analyzed as well. The impurity effect on electric conduction was defined and the energy band models versus concentration and impurity type was proposed as well. In Refs. [11–13], we underlined that description of semiconductors, with MgAgAs ST and their solid solutions belonging to heavily doped and compensated semiconductors, differs from that for traditional semiconductors [14]. In solid solutions with MgAgAs ST, the compositional disorder takes place, whereas long-range order is kept [15]. In amorphous semiconductor model [16], theory of heavily doped and compensated semiconductor assumes that modulation amplitude maximum of the zones of continuous energies is equal to the half of the energy band ($E_g/2$), and the Fermi level (E_F) is localized at the middle of the energy band. We also formulated, with success, the condition to obtain maximal power factor value Z^* [17], which is proven interesting for practical applications, since these intermetallic half-Heusler semiconductors are considered as candidate materials for active elements in thermoelectric generators [18,19]. As reported for these semiconductors [17], the necessary conditions to reach the maximal power factor value is the heavy doping by acceptor or donor impurities with concentrations for which the Fermi level would be fixed close to the mobility edge of valence band or the conduction band. In addition, it should be noticed that during last years, both experimental and theoretical investigations of the well-known Heusler phases delivered new and exciting results on their physical properties.

In this work, we present the investigations of crystal structure and electric transport properties in $Ti_{1-x}V_xNiSn$ solid solutions. Electronic structure calculations, using both the FPLO and the KKR–CPA methods, are performed, and a special attention is paid to analyze V atom influence on thermoelectric characteristics of these compounds.

* Corresponding author.
E-mail address: hlil@grenoble.cnrs.fr (E.K. Hlil).

0022-4596/$ - see front matter © 2010 Elsevier Inc. All rights reserved.
doi:10.1016/j.jssc.2010.09.042

2. Experimental

The $Ti_{1-x}V_xNiSn$ solid solution samples ($x=0$–0.1) were prepared by arc melting using metal elements (Ti, purity 99.97 wt%, Ni—99.99 wt%, and Sn—99.999 wt%, V—99.85 wt%). Synthesis was released under purified Ti-guttered argon atmosphere with non-consumable tungsten electrode on a water-cooled copper hearth. All weight losses were generally less than 1 wt%. Heat treatment of ingots was carried out in vacuum-sealed silica ampoules at 1070 K for 1000 h, followed by quenching in ice water. Crystal structure investigation was performed using X-ray intensities data recorded on HZG-4a diffractometer (Cu K and Cu $K\alpha$-radiation). Lattice parameters were calculated from simple indexing of the patterns. Resistivity (ρ) was measured by two probe dc technique when thermopower (S) was measured in reference to pure copper from 80 to 380 K.

3. Structure electronic calculation details

Electronic and thermoelectric properties of $Ti_{1-x}V_xNiSn$ are investigated by *ab initio* calculations based on the density functional theory. The precise self-consistent full potential local orbital minimum basis (FPLO) method was employed [20,21]. Calculations were processed within the framework of the coherent potential approximation (CPA) which takes the disorder into account. We assumed that the 4*a* (0, 0, 0) and 4*b* (1/4, 1/4, 1/4) sites, occupied by Ni and Sn atoms, respectively, are perfectly ordered whereas the 4*a* (3/4, 3/4, 3/4) site is taken to be randomly shared by Ti and V atoms. Calculations were performed with the scalar relativistic version using the Perdew and Wang exchange–correlation potential. Included valence basis states are 3*spd* and 4*sp* of Ti, V and Ni atoms as well as 4*spd* and 5*sp* of Sn atom. A reciprocal space mesh containing 72 *k*-points within the irreducible wedge of the Brillouin zone was used to perform self-consistent calculations. For comparison, Akai code is used to perform band structure calculations by the KKR method with coherent potential approximation (CPA) in semi-relativistic treatment of core level [22].

4. Results and discussion

We studied the relationship between Z^* values, concentration and doping impurity type, versus substitution of the host Ti ($3d^24s^2$) atoms by V ($3d^34s^2$) ones in the TiNiSn compound. In accordance with the electronic structure of the titanium and vanadium atoms in the $Ti_{1-x}V_xNiSn$ solid solution, the V atom is expected to play the *n*-type impurity role. It should be noticed that in the TiNiSn, ZrNiSn and HfNiSn ternary intermetallics, the donor impurities (defects) exist initially allowing to consider these ternaries as the heavily doped and compensated semiconductors with electron conductivity type.

Crystal structure of TiNiSn ternary compound was refined by powder diffraction method from data obtained with Cu K radiation (Cu $K\alpha$ and Cu $K\beta$) (Fig. 1). Structure refinement showed that TiNiSn crystallizes in MgAgAs ST with $a=0.59270(1)$ nm and $R_I=6.43\%$. However, as shown in Table 1, the site occupation factors (SOF) for Ti and Ni were refined to 0.94 and 0.96. It evidences that TiNiSn stannide has defect structure induced by vacancies in crystallographic positions which can play a role of acceptor impurities.

X-ray diffraction patterns and structure analyses exhibit a single phase for all $Ti_{1-x}V_xNiSn$ alloys (Fig. 2) except for the $Ti_{0.90}V_{0.10}$-NiSn alloy, which contained insignificant amount of additional phases. Lattice parameters for samples, calculated from powder diffraction data, are listed in Fig. 2. At vanadium low concentration ($x=0.005$) and, in spite of the substitution of the greater size host atoms ($r_{Ti}=0.1462$ nm) by the less size impurity atoms ($r_V=0.1346$ nm), a substantial lattice parameter increase was observed. This observed cell parameter increase can be explained in terms of filling the vacancies in initial compound (TiNiSn) where occupation factors are 0.94 and 0.96 for Ti and Ni, respectively. Concentrations of impurity, higher than $x=0.005$, slightly influence the lattice parameter.

Resistivity measurements versus temperature and vanadium content for all samples are reported in Fig. 3. Analysis points to that the resistivity temperature dependences of samples ($x=0$ and $x=0.005$) considerably differ from the rest. Indeed, insignificant substitution of Ti atoms by V ones leads to the insulator–metal transition (i.e. change of conductivity from a semiconductor to metallic-type behavior). Further increase of vanadium concentration

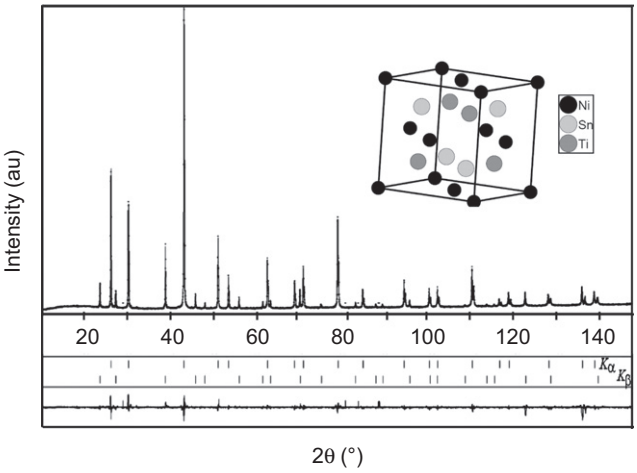

Fig. 1. Observed and calculated diffraction patterns of TiNiSn (model is in the upper right corner) obtained using combined Cu $K\alpha$ and Cu $K\beta$ radiation.

Table 1
Atomic coordinates and isotropic displacement parameters of TiNiSn.

Atoms	Wyckoff positions	*x/a*	*y/b*	*z/c*	SOF	B_{iso} 10^2 nm^2
Ti	4(*a*)	0	0	0	0.94(1)	0.78(5)
Ni	4(*c*)	1/4	1/4	1/4	0.96(1)	0.56(5)
Sn	4(*b*)	1/2	1/2	1/2	1.00(1)	0.47(2)

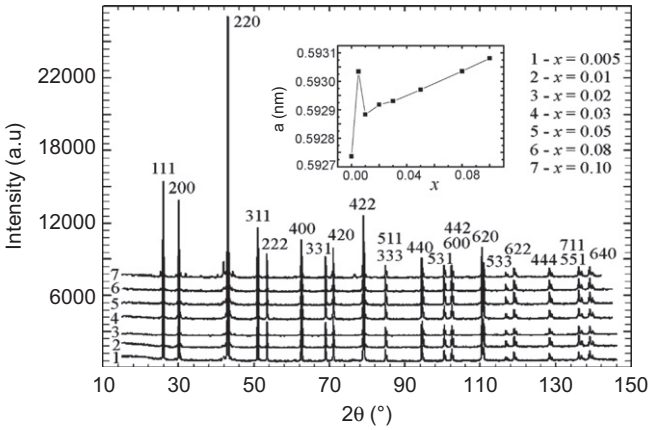

Fig. 2. Diffraction patterns and cell parameters of $Ti_{1-x}V_xNiSn$ solid solution.

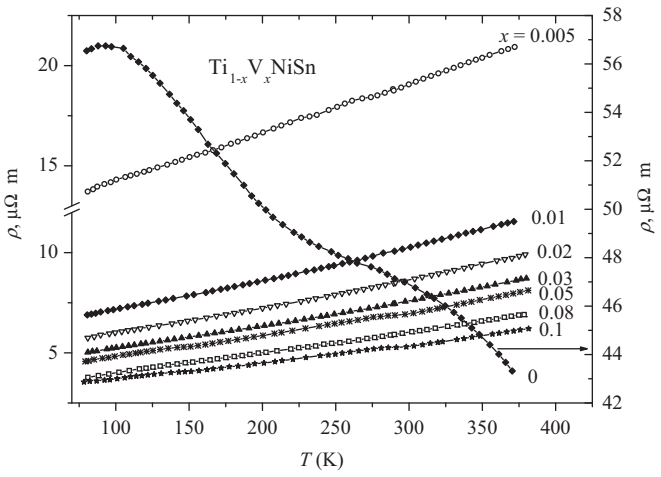

Fig. 3. Temperature dependences of resistivity for $Ti_{1-x}V_xNiSn$ solid solution alloys.

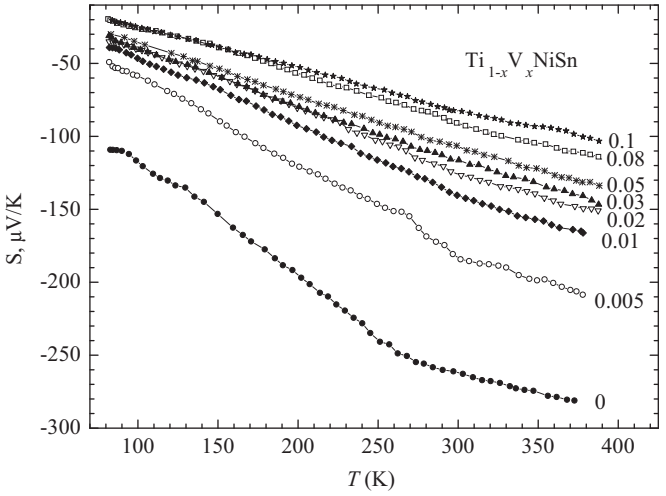

Fig. 4. Temperature dependences of thermopower for $Ti_{1-x}V_xNiSn$ solid solution alloys.

diminishes the ρ value without character change in temperature dependences. Thus, at $x=0.005$, lattice parameter increase and simultaneously sharp change of the transport properties are observed.

As reported in Ref. [23], semiconducting properties of the half-Heusler compounds is determined by two main factors: crystal structure of the MgAgAs-type and host atom type. Analysis of crystal structure of the MgAgAs ST compounds, for example *M*NiSn (M=Ti, Zr, Hf) equiatomic phases displayed in Fig. 1 reveals that the coordination polyhedra of M and Sn atoms are tetrahedrons. That is typical for semiconductor phases as reported in Ref. [23]. Such coordination is determinative in formation of the covalent chemical bonds. These bonds involve $5s^2p^2$ electrons of Sn and $ns^2(n-1)d^2$ electrons of Ti, Zr or Hf. Therefore sp^3- and sd^3-hybridization would take place which leads to the ionic-covalent bonds system in these compounds. These bonds type induces interesting semiconductor properties, and stabilizes the close-packed structure of the MgAgAs type as well. As known, mixed ion-covalent chemical bonds are characteristic for semiconductor compounds, therefore, semiconducting properties are more strongly expressed when covalent bonds contribution is important in crystal. As quoted above, the introduction of insignificant concentration of vanadium in TiNiSn initial semiconductor compound causes the loss of semiconductor properties. This conductivity type change should be accompanied by a sharp reduction of the portion of covalent bonds which can explain the unexpected increase of the unit cell parameter as well.

Temperature and concentration dependences of thermopower of the $Ti_{1-x}V_xNiSn$ alloys are displayed in Fig. 4. They show a decrease of the thermopower value versus V content, without change in its temperature dependence. It is worth noticing that TiNiSn compound is the n-type semiconductor and replacing titanium by the vanadium atoms seems equivalent to introduction of some donor defects in the semiconductor material. As seen in Fig. 4, thermopower sign is not reversed for all concentrations and temperature ranges. Simultaneous analysis from Figs. 3 and 4 show that the gradual increase of vanadium concentration in solid solution consistently results in resistivity and thermopower decrease. This also confirms that the vanadium atoms are donor doping in the $Ti_{1-x}V_xNiSn$ solid solution. Thus, the Fermi level shifts to the bottom of the conduction band and moves towards higher energies when V content increases.

We also are interested in the power factor for which temperature and concentration dependences are reported in Fig. 5. As seen, the power factor increases versus temperature and when vanadium

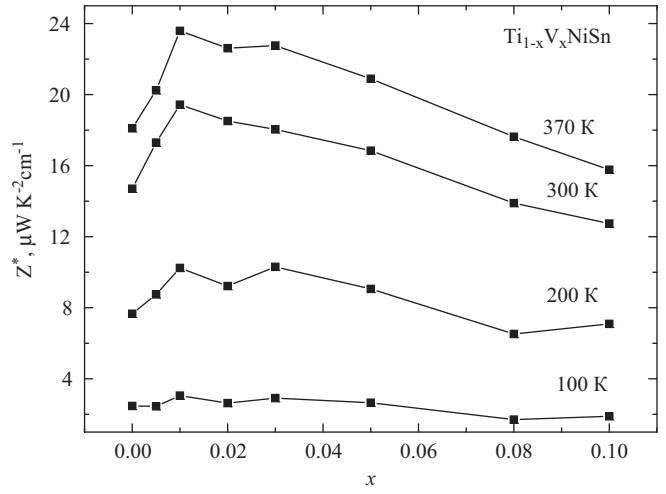

Fig. 5. Composition dependences of power factor at different temperatures for $Ti_{1-x}V_xNiSn$ solid solution alloys.

content x varies, a maximum is observed at $x=0.01$. It was stated from Ref. [17] that the main condition of achievement of maximal values of the power factor in any materials based on of MgAgAs ST compounds was the strong doping of the ternary compounds by acceptor and/or donor impurities, for which the Fermi level is fixed by the mobility edge of the valence band or conduction band. As conclusion from our experiment point of view, it is reasonable to assert that in the $Ti_{1-x}V_xNiSn$ solids the Fermi level crosses the conduction band at vanadium concentration equal to 0.01.

Examination of these half-Heusler phases based on the MgAgAs ST intermetallic compounds allows to conclude that if the type of doping was such that leads to overcompensation of the semiconductor and to sign reversal of main charge carrier, we reach the maximal values of the power factor at certain concentration of impurity. However, this value in most cases is less for undoped semiconductor [24,25]. It is also ensued that the highest value of the power factor is reached when doping the intermetallic semiconductor by impurity type which agree with the type of main charge carriers. Data of presented article (Fig. 5) exhibit that doping of the *n*-TiNiSn intermetallic semiconductor by the vanadium

donor impurity leads to a considerable increase of the power factor reference to undoped ternary compound.

Now, we will be interested in the electronic structure calculations to see how these experimental results will agree with theoretical conclusions. Total density of states (DOS), deduced from the band structure calculations versus V content, is presented in Fig. 6. First, DOS close to the Fermi level gives evidence of a small gap presence for TiNiSn. The gap width is estimated to be about 0.7, 0.5 and 0.45 eV for $x=0$, 0.05 and 0.1, respectively. Taken as a reference energy, Fermi level position in the gap points out to a thermoelectric character i.e. a semi-conducting-like state that correlates the resistivity decrease versus temperature ($d\rho/dT<0$) when $x=0$.

Calculations confirm the Fermi level shift to the band conduction when Ti atom is progressively substituted by V atom, as expected from our experimental data. This shift is understood in terms of the electron number increase in the valence band. Transition from semiconducting-like state (E_F falls in the gap for $x=0$) to metal-like state (E_F in the BC when x increases) is confirmed as well. This transition does not involve the Seebeck coefficient value reversal, since Fermi level shifts from gap to conduction band. Chemical bonding analysis, based on calculated

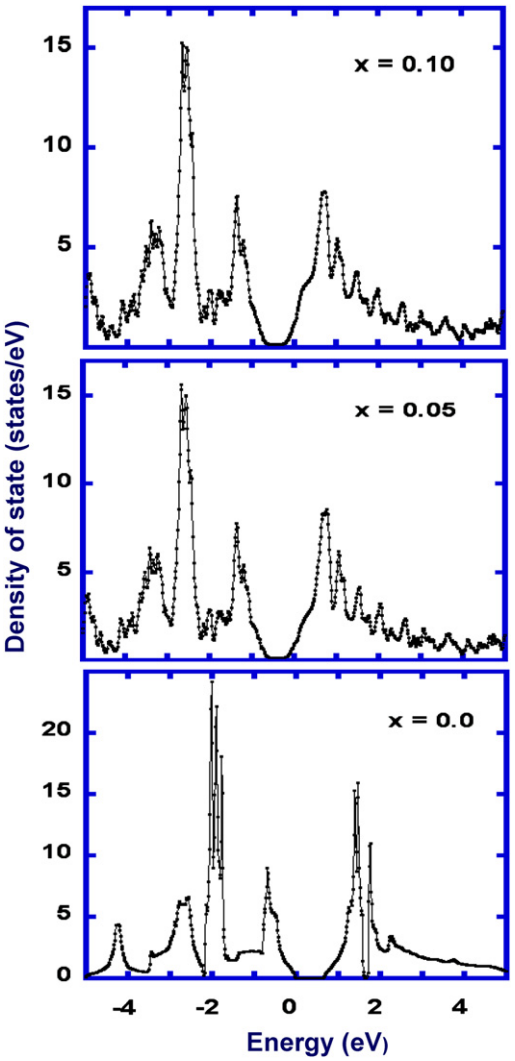

Fig. 6. Total DOS of $Ti_{1-x}V_xNiSn$ solid solution alloys. For comparisons versus concentration, the DOS is shifted on Y-axis by 25 and 40 for $x=0.05$ and 0.10, respectively.

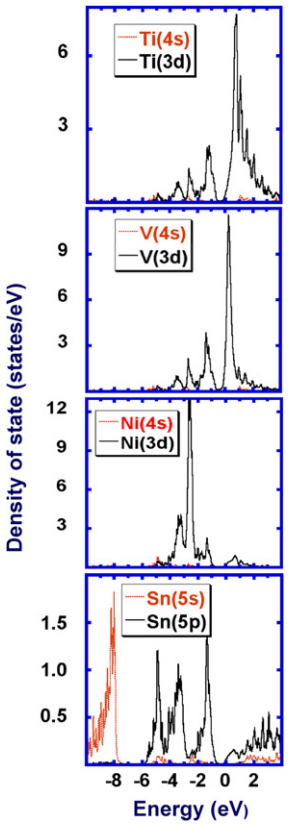

Fig. 7. The l-decomposed DOS of like-states s, p and d of Tl, V, Sn and Ni in $T_{0.95}V_{0.05}NiSn$ solid solution alloys.

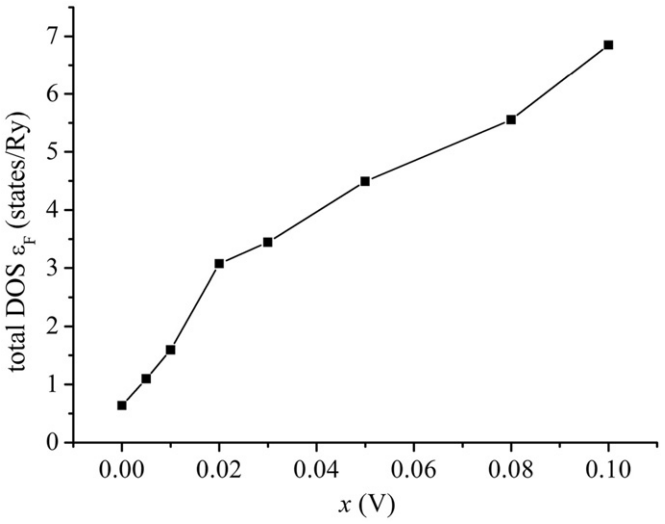

Fig. 8. Composition dependence of the density of states at Fermi level (KKR-CPA method).

Mulliken electron populations, indicates that, for $x=0$, the net charge is $-1.31|e|$, $+1.07|e|$, and $+0.23|e|$ on Ti, Ni and Sn atoms, respectively. These values indicate a charge transfer between atoms in undoped TiNiSn. When V atoms are introduced, the calculated total charge atomic values, found to be insensitive to the V content, are 21.81, 28.57 and 49.62 for Ti, Ni and Sn, respectively. Small charge transfer is evidenced since these values are slightly different from neutral charge atomic ones 22, 28 and 50 for Ti, Ni

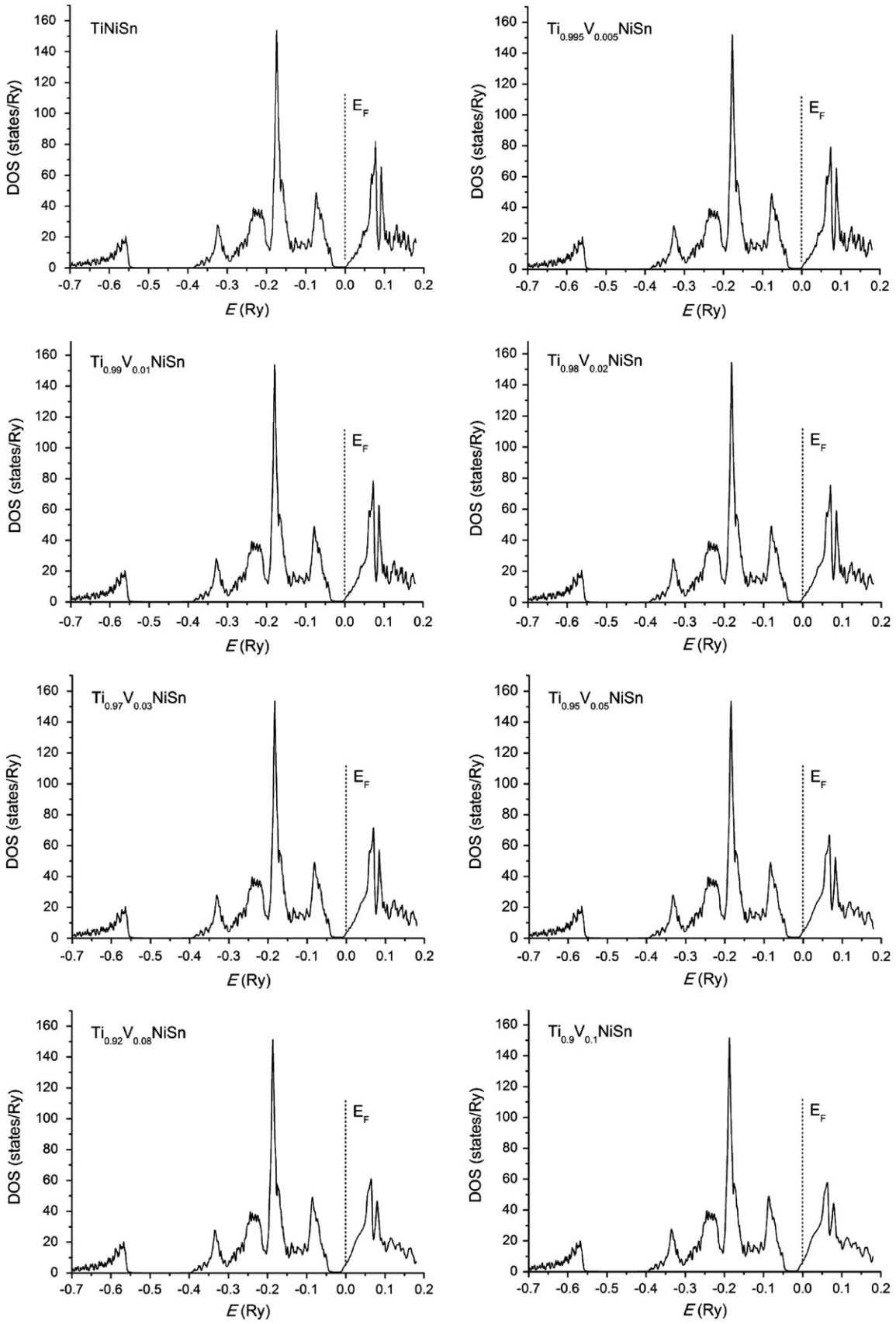

Fig. 9. Total DOS of $Ti_{1-x}V_xNiSn$ solid solution alloys obtained with KKR method.

and Sn isolated atoms, respectively. The *l*-decomposed DOS of like-states *s, p* and *d* of Ti, V, Sn and Ni in $Ti_{0.95}V_{0.05}NiSn$ solid solution alloys are presented in Fig. 7. The specify that total DOS is mainly originating from Ni(3*d)* band contributions in valence band whereas V(*3d*) and Ti(*3d*) bands contribute to the unoccupied states. DOS contributions from Sn to both occupied states and unoccupied states are found weak reference to those of the remaining atoms.

These FPLO calculations are compared to the calculations using the KKR–CPA method. This choice is due to the fact that this second method is widely used to investigate the electronic and magnetic properties of such *half-Heusler materials* [26–29]; hence it could assert our theoretical conclusions. The KKR–CPA calculations show that, whatever V content, Fermi level is situated at the edge of the conduction band. Contrary to the FPLO method, this method gives, particularly for $x=0$, correct Fermi level position which is situated near conduction band. It indicates n-type of conductivity which fully agrees with the experiment. Progressive substitution of Ti by V atom increases the density of states on the Fermi level (Fig. 8) and shifts it into the conduction band (Fig. 9).

It should be noticed that our calculations include our measured lattice parameter change versus vanadium concentration in cubic system having atoms on special sites (0, 0, 0), (1/4, 1/4, 1/4) and (3/4, 3/4, 3/4). Therefore, inter atomic distances change are included in calculations, since these distances are proportional to the lattice parameter. As a consequence, when Ti is progressively substituted by V, both charge change and the size effect induced by V substitution are considered.

5. Conclusions

Based on experimental and calculation approaches, crystal structure, temperature and concentration dependences of the resistivity and thermopower of $Ti_{1-x}V_xNiSn$ substitutional solid solution are investigated. It is underlined that V atoms behave as donor impurity in this semiconductor, and low V concentration ($x=0.005$) in $Ti_{1-x}V_xNiSn$ solid solution results in the insulator–metal transition (i.e. change of the conduction type from a semiconductor to metallic-like). Doping by such impurity having the same type as the basic charge carriers leads to power factor increase in the $Ti_{1-x}V_xNiSn$ thermoelectric alloys.

Electronic structure calculations give a complete picture about understanding thermoelectric properties since they confirm all experimental data assertions. They mainly highlight insulator–metal transition, negative sign of thermopower and vanadium behaves as donor.

Acknowledgment

This work is supported by Department of Education and Science of the Ukraine, Grant no. 0109U002069.

References

[1] Yu.V. Stadnyk, R.V. Skolozdra, Izv. Akad. Nauk SSSR, Neorgan. Mater. 27 (1991) 2209.
[2] Yu.V. Stadnyk, R.V. Skolozdra, Metals 1 (1994) 164.
[3] Yu. Stadnyk, L.P. Romaka, J. Alloys Compd. 316 (2001) 169.
[4] F.G. Aliev, N.B. Brandt, V.V. Kozyrkov, V.V. Moshchalkov, R.V. Skolozdra, Yu.V. Stadnyk, V.K. Pecharsky, Pisma v ZhETF 45 (1987) 535.
[5] F.G. Aliev, A.I. Belogorokhov, N.B. Brandt, V.V. Kozyrkov, R.V. Scolozdra, Yu.V. Stadnyk, Pisma v ZhETF 47 (1988) 151.
[6] R.V. Skolozdra, Yu.V. Stadnyk, L.P. Romaka, F.G. Aliev, J. Thermoelectricity 3 (1994) 29.
[7] H. Hohl, A. Ramirez, C. Goldmann, G. Ernst, B. Wölfing, E. Bucher, J. Phys.: Condens. Matter 11 (1999) 1697.
[8] Q. Shen, L. Chen, T. Goto, T. Hirai, J. Yang, G.P. Meisner, C. Uher, Appl. Phys. Lett. 79 (2001) 4165.
[9] S. Katsuyama, H. Matsushima, M. Ito, J. Alloys Compd. 385 (2004) 232.
[10] K. Kurosaki, H. Muta, S. Yamanaka, J. Alloys Compd. 384 (2004) 51.
[11] Yu.V. Stadnyk, V.A. Romaka, Yu.K. Gorelenko, L.P. Romaka, D. Fruchart, V.F. Chekurin, J. Alloys Compd. 400 (2005) 29.
[12] Yu. Stadnyk, V.A. Romaka, M. Shelyapina, Yu. Gorelenko, L. Romaka, D. Fruchart, A. Tkachuk, V. Chekurin, J. Alloys Compd. 421 (2006) 19.
[13] V.A. Romaka, Yu.V. Stadnyk, M.G. Shelyapina, D. Fruchart, V.F. Chekurin, L.P. Romaka, Yu.K. Gorelenko, Semiconductors 40 (2006) 131.
[14] B.I. Shklovskii, A.L. Efros, Zh. Eksp. Teor. Fiz. 61 (1971) 816;
B.I. Shklovskii, A.L. Efros, Sov. Phys. JETP 34 (1971) 435.
[15] Yu. Kh Vekilov, Soros Educ. J. 6 (1999) 105.
[16] B.I. Shklovskii, A.L. Efros, Zh. Eksp. Teor. Fiz. 62 (1972) 1156;
B.I. Shklovskii, A.L. Efros, Sov. Phys. JETP 35 (1972) 610.
[17] O.I. Bodak, V.A. Romaka, Yu.K. Gorelenko, M.G. Shelyapina, Yu.V. Stadnyk, L.P. Romaka, V.F. Chekurin, D. Fruchart, A.M. Gorin, Phys. Chem. Solid State 7 (2006) 76.
[18] G.S. Nolas, J. Poon, M. Kanatzidis, MRS Bull. 31 (2006) 199.
[19] A.V. Shevel'kov, Russ. Chem. Rev. 77 (2008) 1.
[20] K. Koepernik, H. Eschrig, Phys. Rev. B 59 (1999) 1743.
[21] K. Koepernik, B. Velicky, R. Hayn, H. Eschrig, Phys. Rev. B 55 (1997) 5717.
[22] MACHIKANEYAMA2002v09: H. Akai, Department of Physics, Graduate School of Science, Osaka University, Machikaneyama 1-1, Toyonaka 560-0043, Japan. akai@phys.sci.osaka-u.ac.jp.
[23] R.V. Skolozdra, Stannides of rare earth and transition metals (in Ukrainian), Lviv, Svit, (1993) 200.
[24] Yu. Stadnyk, Yu. Gorelenko, A. Tkachuk, A. Goryn, V. Davydov, O. Bodak, J. Alloys Compd. 329 (2001) 37.
[25] V.A. Romaka, D. Fruchart, Yu.V. Stadnyk, J. Tobola, Yu.K. Gorelenko, M.G. Shelyapina, L.P. Romaka, V.F. Chekurin, Semiconductors 40 (2006) 1275.
[26] V.A. Dinh, K. Sato, H. Katayama-Yoshida, J. Phys. Soc. Jpn. 77 (2008) 14705.
[27] T. Fukushima, K. Sato, H. Katayama-Yoshida, P.H. Dederichs, J. Phys. Soc. Jpn. 76 (2007) 94713.
[28] K. Sato, L. Bergqvist, J. Kudnovsky, P.H. Dederichs, O. Eriksson, I. Turek, B. Sanyal, G. Bouzerar, H. Katayama-Yoshida, V.A. Dinh, T. Fukushima, H. Kizaki, R. Zeller, Rev. Mod. Phys. 82 (2010) 1633.
[29] H. Katayama-Yoshida, K. Sato, M. Toyoda, V.A. Dinh, T. Fukushima, H. Kizaki, in: Handbook of Spintronic Semiconductors, Pan Stanford Publishing Pte Ltd., 2009 Chapter 1 (2010) 1.